Quantifying water release into the soil from water absorbing polymers under drought conditions

Abhisekh Saha[1]; Sreedeep Sekharan[2]; Uttam Manna[3]; Snehasis Tripathy[4]

[1]Assistant Professor, Department of Civil Engineering, Malaviya National Institute of Technology Jaipur, Rajasthan, India, email: abhisekhsaha.ce@mnit.ac.in (Corresponding author)

[2]Professor, Department of Civil Engineering, Indian Institute of Technology Guwahati, India, email: srees@iitg.ac.in

[3]Professor, Department of Chemistry and Centre for Nanotechnology, Indian Institute of Technology Guwahati, India, email: umanna@iitg.ac.in

[4]Professor, School of Engineering, Cardiff University, Queen's Buildings, West Grove, Newport Road, Cardiff CF 243AA, UK, email: tripathys@cardiff.ac.uk

Abstract

The use of water absorbing polymers (WAPs) is evolving as an amicable solution for preserving soil moisture and promoting vegetation cover under extreme drought conditions associated with changing climate. WAPs can absorb significant amount of irrigation/rainwater and release water to soil when moisture deficit occurs. As compared to the water absorbing characteristics, comprehensive information on the water release characteristics of WAPs when interacting with various soil types is scarce in the literature. The objective of this study is to develop an experimental methodology for understanding the water release characteristics (WRCs) of different WAPs in various soils. A horizontal soil column test (HSCT) setup was used for studying the WRCs of two WAPs [fly ash-derived WAP (FA-WAP) and commercially available acrylic-based WAP (Com-WAP)] in three different soils (sand, silt loam, and clay loam). The tests were conducted on dry soils and with the WAPs at two initial conditions, including fully hydrated conditions and limited water availability conditions. A two-parameter kinetic equation was found suitable for quantifying the water release characteristics of the WAPs both in (a) soils and (b) atmosphere. The study revealed that the dry soils in contact with the FA-WAP able to quickly achieve more than 95% saturation within 12 hours whereas the dry soils in contact with Com-WAP remain well below full saturation after the same time interval. The different combinations of soils and WAPs suggests better efficiency of FA-WAP and clay loam soil for higher WRC if sufficient amount of water is available in WAP. The water release rate from FA-WAP to dry soil was found to be much higher than the Com-WAP during initial stage. Under the limited water availability conditions, FA-WAP was able to release 97% of the total absorbed water to the initially dry soils as compared to Com-WAP where 90% of the stored water was released.

Keywords: Moisture release; Horizontal soil column test; Soil texture; Kinetics equation; Climate action

Introduction

Climate change-induced water stress impacts various civil and environmental engineering projects, such as highway embankments, green infrastructures, vegetated landfill covers, and bioengineered slopes (Bordoloi et al. 2020; Liu et al. 2021; Pk et al. 2021). The rise in mean global temperature and frequent droughts cause soil drying, generation of desiccation cracks, soil erosion, and poor soil health (Kandalai et al. 2023). Long-term effects of drought condition (i.e., prolonged drying condition) alter soil hydraulic characteristics (infiltration, permeability and soil-water retention) and hydrological process with a negative impact on the stability of geotechnical infrastructures (Vardon 2015). There is a need to develop different climate-resilient technologies to minimize the negative influence of climate change on available soil-water.

Soil amendment through innovative materials (biomaterials, polymer composites, nanomaterials) is one of the approaches to control the loss of soil water and its conservation in the vadose zone thereby promoting vegetation cover (Sreedeep et al. 2019; Saha et al. 2021c; Ni et al. 2024). Water absorbing polymers (WAPs), or superabsorbent hydrogels are emerging as a low-cost and eco-friendly materials for improving the water retention characteristics of the soils under arid conditions (Hussien et al. 2012; Cao et al. 2017; El-Asmar et al. 2017; Saha et al. 2022b). The WAP is capable of absorbing and storing water more than 100 times its own weight in its polymer structure and exhibit volumetric expansion (Saha et al. 2020b; Saha et al. 2021a). The stored water in the WAP is released into the dry soil, thereby maintaining vegetation growth for a prolonged duration under drought condition. Recent studies have shown that biodegradable WAPs could be developed from various waste products, such as starch, cellulose, chitosan, fly ash, and alginate (Rodrigues et al. 2012; Spagnol et al. 2012; Mignon et al. 2019; Sarmah and Karak 2019; Saha et al. 2020c), which makes them ideal material as soil conditioners with minimal environmental impact.

The water-absorption capacity (WAC) and swelling characteristics of WAP can vary depending on their composition and the electrical conductivity of hydrating fluid (Saha et al. 2021b). The practical application of a WAP depends on (a) how much water it can absorb, (b) how inclusion of WAP contributes to the enhancement of water retention characteristics of the soil, and (c) how much of the stored water in the WAP can be released into the different soil types when water deficit occurs. Most of the previous studies focused on the first two aspects of WAP-soil interaction, where the influence of WAP on soil-water retention characteristics (SWRC), hydraulic conductivity, and infiltration characteristics of soil has been investigated by uniformly mixing dry WAP particles in soils. Narjary et al. (2012) indicated an improvement in SWRC of different soil texture due to the addition of hydrophilic polymers. Zhao et al. (2020) conducted laboratory tests to compare the water evaporation rate of different hydrophilic polymers into the atmosphere. Saha et al. (2021a) proposed a model for predicting the drying SWRC of WAP amended soil using modified phase relationship of WAP-soil system. Saha et al. (2022a) studied the SWRCs of WAP amended soils subjected to multiple drying-wetting cycles and proposed a predictive model to estimate wetting SWRC from the measured drying SWRC. Adjuik et al. (2022) showed a decrease in the saturated hydraulic conductivity of soil amended with lignin-based hydrophilic polymer. It was noted from these studies that the flow mechanism at the WAP-soil interface requires separate WAP and soil layers instead of uniform mixes of WAP and soils. Saha et al. (2022b) developed a horizontal diffusion cell to study the moisture diffusivity from a commercially available WAP to dry soil. The moisture diffusivity through the soil column was found to be similar to the moisture diffusivity values estimated from wetting SWRC.

The existing studies have majorly focused on improving the WAC of the WAP through innovation in polymerization techniques, and usage of different hydrophilic monomers, and quantifying the hydraulic characteristics (i.e., hydraulic conductivity, SWRC, infiltration

properties) of WAP amended soil. However, none of these studies have focused on the water release characteristic (WRC) of different WAPs in different soil types. When WAP is mixed with the soil, it is impossible to quantify water release from WAP to soil because once it is mixed, WAP cannot be separated for water content measurement. One possible way to quantify water release from WAP to soil is to provide it as layer so that the water content variation with time can be measured accurately. Such a quantification of water release of WAP is a pre-requisite for selecting WAP for field applications. The knowledge of WRC of WAPs is also required to ensure efficacy of WAP-soil systems in the conservation of soil moisture during drought conditions. It helps to quantify how much of the stored water in the hydrated WAP can be released into the dry soil. In this context, the WRC of hydrated WAP into both (a) free atmosphere and (b) soil are required for several applications, such as in bioengineered slopes, urban green infrastructures, and arid/ semi-arid agriculture.

Krasnopeeva et al. (2022) reported the in-situ applications of various WAPs as water and nutrient storage, and retention materials. The rate of WAP required for increasing seed and dry matter yields and urea release characteristics have been shown to depend on plant types. Past studies have stated that the in-situ performance of WAPs may be influenced by the plant type, water quality, temperature, and chemical interactions (Bo et al. 2012; Cao et al. 2017; Dehkordi 2018; Yang et al., 2020b). Therefore, studies of the water release characteristics of different WAPs when interacting with different soil types are crucial for the selection of WAPs for field applications. A study on the water movement dynamics of WAPs in field conditions is beyond the scope of the present study.

The objective of this study is to develop an experimental methodology and for understanding the WRCs of different WAPs with different soil types. The present study critically comprehends the performance of two different WAPs, including a commercial WAP (Com-WAP) and in-house developed fly ash modified WAP (FA-WAP), in three different soil

types (i.e., sand, silt loam, and clay loam). The WRC of both the WAPs were evaluated under controlled laboratory condition, where the water release is dependent only on soil and WAP characteristics. The total quantity of water transferable from WAP to dry soil was further studied by varying the layer thickness of WAP in HSCT.

Materials and methodology

Materials

Soil

Three natural soils were collected from diverse locations in the Northeastern region of India. The collected soils were air-dried and sieved through the Indian Standard (IS) sieve size of 2 mm. The soils were further characterized for their basic physical properties, such as particle size distribution (PSD) curve, specific gravity, hygroscopic water content, consistency limits, and cation exchange capacity (CEC), following the guidelines provided in ASTM standards (ASTM 2007; ASTM 2014; ASTM 2015; ASTM 2017b; ASTM 2018) (Table 1). The soils were classified based on the Unified Soil Classification System (USCS) [ASTM 2017a] and the United States Department of Agriculture (USDA). The soil mineralogical composition was characterized using X-ray diffraction (Rigaku, MicroMax, Tokyo, Japan) and reported in Table 1.

Water absorbing polymer (WAP)

A commercially available WAP (Com-WAP) along with a laboratory developed fly ash modified water absorbing polymer (FA-WAP) were used in this study (Fig. 1). The selected Com-WAP (Stockosorb) is a partially neutralized potassium polyacrylate compound, manufactured by Evonik Industries, Germany. The laboratory-grade FA-WAP was prepared by grafting an industrial solid waste material, fly ash (FA), onto the polymer chain of partially neutralized sodium polyacrylate (details presented in Saha et al. 2020c). Both the WAPs were

systematically characterized for their functional groups, elemental compositions, equilibrium water-absorbing capacity, and equilibrium swelling time (Table 2). The functional groups of both WAPs were characterized with Fourier transform infrared (FTIR) spectrophotometer (Perkin Elmer, Spectrum Two, Waltham, MA) by using potassium bromide (KBr) pellet method. The FTIR analysis of both Com-WAP and FA-WAP showed the presence of intermolecular stretching vibration of hydroxyl and carboxyl groups (Saha et al. 2020a, c). An additional peak was observed in FA-WAP due to the presence of asymmetrical and symmetrical stretching vibration of Si—O—Si bond, which are characteristic peaks of fly ash (Saha et al. 2020c). The elemental compositions of the WAPs were determined using the FESEM-EDS analysis (Zeiss Sigma, Oberkochen, Germany). The elements of Com-WAP were found to be oxygen, carbon, potassium, and nitrogen, whereas the elements of FA-WAP are oxygen, carbon, sodium, silicon, calcium, aluminium, and nitrogen. The existence of potassium (K) in Com-WAP confirms the potassium polyacrylate compound whereas the existence of Si, Al confirms the presence of alumino-silicate compound (i.e., fly ash) in FA-WAP. The equilibrium water-absorbing capacity and equilibrium swelling time of the WAPs were measured by following the procedure described in the literature (Saha et al. 2021b). The dry WAP was kept inside a nylon tea bag, and its WAC (g/g) at different time intervals was measured by immersing it in distilled water. The procedure was continued till the WAP reached its equilibrium maximum swelling, and the obtained values are reported in Table 2.

Methodology

Water release from WAP to atmosphere

The water release from WAP to ambient atmosphere is quite important for understanding the release behaviour of WAPs when it is not interacting with any other porous medium. It can be noted that the water release from WAP to soil (or any other porous medium) can be governed by several properties of soil, such as pore-size distribution, porosity,

mineralogical composition, hydraulic conductivity, etc. Therefore, an evaporation experiment was conducted in the controlled laboratory conditions (temperature= 25°C; relative humidity = 50%) using the selected WAPs before delving into the complex WAP-soil systems. The loss of water from hydrated WAP to the atmosphere was quantified in terms of change in gravimetric water content (GWC) of WAP as a function of time. For this purpose, 1g of dry WAP was added to the required amount of distilled water to achieve maximum swelling equilibrium conditions. The swollen sample was placed in a glass disc (diameter = 100 mm), and allowed to dry under controlled laboratory conditions. The water release kinetics (to free atmosphere) was determined by noting the weight of the swollen WAP sample at regular time interval until there was no reduction in weight with time (completely air-dried). Five identical samples were prepared both for FA-WAP and Com-WAP for the weight measurement to ensure the repeatability of the measured data. The experimentally measured water release kinetics of hydrated WAP was fitted to the two parameters empirical model (Eq. 1) proposed by Peleg (1988) for describing water release from high swelling materials.

$$w_t = w_0 - \frac{t}{k_1 + k_2 t} \tag{1}$$

Here, w_0 is the initial GWC (g/g) of fully hydrated WAP (equilibrium swelling); w_t is the GWC (g/g) of hydrated WAP at time t after drying is initiated; k_1 and k_2 are kinetics constant and characteristic constant, respectively. The rate of water release (Eq. 2) can be obtained by differentiating Eq. (1) with respect to time as follows,

$$\frac{dw_t}{dt} = -\frac{k_1}{(k_1 + k_2 t)^2} \tag{2}$$

A similar glass disc, filled with distilled water was also placed adjacent to the hydrated WAP to compare the evaporation of water from the hydrated WAP and free water surface. The water evaporation rate (ER) was computed from Eq. (3) for a better comparison of water release characteristics under WAP-atmosphere interaction (Yang et al. 2020a).

$$ER\ (mm/hr) = \frac{Amount\ of\ water\ evaporated\ per\ hour\ (mm^3/hr)}{Cross\ sectional\ area\ of\ container\ (mm^2)} \quad (3)$$

It may be noted that the ER calculation of hydrated WAP involves the measurement of cross cross-sectional area of the container. To avoid the error in the cross-sectional area measurement, the container was tamped to spread the hydrated WAP over the entire surface area after every weight measurement.

Water release from hydrated WAP to dry soil

Water release from hydrated WAP to dry soil is an important aspect to consider for the application of WAP in actual field conditions. In actual scenarios, the WAP particles are uniformly mixed with the soil and it is difficult to characterize the water release characteristics (WRC) for different soil-WAP combinations. The present study considered two different cases to evaluate the WRC, including (i) fully hydrated WAPs and unsaturated soils (i.e., air-dry soil) and (ii) hydrated WAPs with limited water availability and unsaturated soils. A series of horizontal soil column tests were conducted in a transparent cylindrical acrylic tube with an internal diameter of 20 mm and length of 110 mm (Saha et al. 2022a). Air-dried soils were hand compacted to the cylindrical tube to a thickness of 80 mm. The initial packing compaction states of the soil samples are tabulated in Table 3. The direct interaction of soil and hydrated WAP was avoided by placing a filter paper in between soil and WAP layers. A 30 mm thick layer of hydrated WAP was packed on top of the filter paper. The thickness of the hydrated WAP (i.e., 30 mm) was selected based on the saturated volumetric water content (= porosity) of the red soil (RS) sample to allow near saturation of all the soil samples. It can be noted that RS sample has higher porosity as compared to the other two soils and therefore, RS require higher water to achieve complete saturation. After placing the hydrated WAP, the cylindrical tube was immediately sealed from the top and placed horizontally allowing water migration from hydrated WAP to dry soil. This setup ensures that there is no loss of water to the

atmosphere, and there is release of water from hydrated WAP to dry soil under zero gravitational head. Due to water release from the hydrated WAP, the wetting front advances through the horizontal soil column, as shown in Fig. 2. Multiple columns with identical initial states were arranged for a given soil-WAP combination. Depending on the wetting front advancement rate, horizontal tubes were dismantled at predetermined times to establish the moisture profile [i.e., volumetric water content (VWC) at different distances from the WAP-soil interface and time]. For each time intervals, five identical samples were dismantled and the GWC was measured to check the repeatability of the measured data. For the measurement of gravimetric water content (GWC), a small amount of soil was scooped out from the soil-WAP interface and at every 10 mm distance from the interface. The GWC value was multiplied by the dry density to obtain the VWC of the soil sample.

The water release from hydrated WAP to initially air-dried soil is governed by two factors, (a) initial soil suction in air dried sample and (b) water migration through the soil layers, as explained in Fig. 3. The magnitude of initial suction corresponding to air dry state of the soil determines the entry of water into the soil at the interface. A high suction gradient exists at the interface due to negligible suction in hydrated WAP (fully saturated) and high suction in air-dried soil (Saha et al. 2021c). It may be noted that the magnitude of initial suction corresponding to air dried state depends on soil type and presence of fine particles (Fredlund and Rahardjo 1993). The water entered at the soil interface gets redistributed in the soil layer (Saha et al. 2022a). The rate of water redistribution further determines the subsequent rate of water release from the hydrated WAP to the soil. If the rate of water migration in soil column is low, then the redistribution of water from the interface will be less. This causes near-steady state saturation adjacent to the interface. Due to this, the suction gradient decreases thereby reducing the rate of water entry into the soil. If the rate of water migration is high, then the redistribution will be faster resulting in a continuous transient water entry at the interface. As

the soil saturation increases with time, the suction gradient between the WAP and soil reduces thereby decreasing the water entry.

For quantifying WRCs of WAPs, the weight of hydrated polymer was measured at different time intervals when horizontal columns were dismantled. The reduction in weight of the hydrated WAP was measured until the soil attained the saturated water content or there was no appreciable reduction in the weight of WAP with time. For the measurement of hydrated WAP weight, five repetitions were performed to check the repeatability of the measured data. The weight reduction in hydrated polymer represents the amount of water transferred from WAP to the soil. The measured data was used to represent the WRCs of WAPs in terms of GWC and elapsed time. In addition, the water release rate from both the WAPs to dry soil was calculate ed using Eq. (2) to understand the effect of soil properties and WAP properties individually. Furthermore, efforts were made to evaluate the WRC under limited availability of water. This was achieved by placing 20 mm and 10 mm thick layer of hydrated WAPs in contact with the used dry soils (FS, BS, and RS) packed in HSCT. Restricting the thickness of hydrated WAP ensured water availability less than the quantity required for complete saturation of the soil samples. These measurements were needed to determine the percentage of absorbed water that can be released into the dry soil from WAP when limited water is available.

Results and Discussion

Water release due to evaporation resulting from WAP-atmosphere interaction

The water release kinetics of the Com-WAP and FA-WAP exposed to the atmosphere are presented in Fig. 4(a). The change in GWC due to evaporation ranging from an equilibrium swelling state to a completely dry state was measured. This information is important because the WAP close to the soil surface can lose water by evaporation and further help to understand

the water release of hydrated WAP individually without considering the influence of soil type. It can be observed that the Com-WAP and FA-WAP took 400 hrs and 520 hrs, respectively, for complete desaturation. The higher desaturation time in FA-WAP than Com-WAP can be due to the higher equilibrium water-absorbing capacity and lower water release rate of the former. The water absorption and desaturation characteristics of FA-WAP in the study are similar to that reported by Chang et al. (2021). The higher desaturation time in FA-WAP was verified by fitting the water release kinetic equation (Eq. 1) to the experimental data. The values of parameters (k_1, k_2) are summarized in Table 4. The value of the characteristic constant (k_2) was found to be independent of WAP type. A larger value of k_1 for FA-WAP indicates that the loss of water content (water release) from FA-WAP to the free atmosphere was less compared to Com-WAP. This is advantageous for FA-WAP because the WAP is expected to have low water loss (evaporation) to the atmosphere.

The variation in evaporation rate (ER) with time for both WAPs and free water was calculated and compared in Fig. 4(b). As expected, it can be observed that the water evaporation rate from hydrated WAP was less than free water evaporation. This is mainly due to the fact that the absorbed water molecules inside the polymer structure are attached to the hydrophilic groups through intermolecular hydrogen bonds (Shah et al. 2018). While the ER remains constant for free water, there are three distinct phases of water evaporation for hydrated WAP. The ER is maximum during the first stage (Phase I) and remains constant for the entire stage. The second phase of evaporation begins with a sharp decrement in ER, which can be attributed to the air entering the WAP matrix. Due to the progressive reduction in WAP water content, the ER also decreases with time. In the final phase, the ER becomes minimal (near zero) as the sample has already reached its residual state. In this state, the limited residual water is tightly attached to the polymer structure, and it cannot be extracted at ambient temperature. From Fig. 4(b), it is quite evident that the ER is lower in FA-WAP than Com-WAP (phase I). Also, the

duration of phase I is less in Com-WAP than FA-WAP, which means quick air entry. This indicates that FA-WAP releases the stored water to the atmosphere at a lower rate than Com-WAP and the release continues for a longer duration. This is an advantage of FA-WAP compared to Com-WAP.

As stated above, the ER versus time response showed 'S' shaped variation and hence, a sigmoidal equation [similar to van Genuchten model (1980)] (Eq. 4), that represents the evaporation loss characteristic curve (ELCC) for WAP was fitted to the observed ER versus time data and the parameters are summarized in Table 5. This ELCC can be used to define the evaporation loss characteristics of WAP under controlled evaporation at a reference temperature, and humidity condition (25 °C and 50% RH).

$$ER(t) = ER_r + \frac{ER_s - ER_r}{\left[1+\left(\frac{a}{t}\right)^n\right]^m} \quad (4)$$

ER(t) represents the evaporation rate at time, *t;* ER_r is the residual evaporation rate; ER_s is the evaporation rate at the saturated stage (equilibrium swollen WAP); *a*, *n*, and *m* are curve fitting parameters.

The fitting parameter (ER_s) presented in Table 5 also indicates a higher ER of Com-WAP than FA-WAP in the saturated state. The rate of water release parameter (*n*) is higher for Com-WAP indicating a higher desaturation rate of Com-WAP than FA-WAP to the atmosphere. The results suggest that these curve-fitting parameters of ELCC can be used for comparing the performance of hydrated WAPs exposed to the atmosphere. The comparison can be used for initial screening and selection of WAP for further application in the soil.

Water release from hydrated WAP to dry soil

Water movement through the horizontal soil column

The variation of wetting front distance (x_f) from the WAP-soil interface was acquired by visual inspection at various interval of time and presented in Fig. 5. There is a specific and consistent trend for wetting front advancement in soils corresponding to both the WAPs. For Com-WAP and FS interaction, the time taken for the wetting front to advance 7.6 cm was 32 hrs whereas for FA-WAP and FS interaction, it was 7.7 cm in 12 hrs. It can be noted that water movement through soil layer is influenced by both soil type and composition of WAP. The influence of soil texture on the wetting front advancement rate observed in this study agreed well with the trends reported in the literature (Liu et al. 2009; Villarreal et al. 2019). The higher wetting front advancement rate in coarse-grained soils is due to its high permeability associated with larger pore structure and low tortuous flow path. It was found that the water entry and redistribution through initially dry soil is faster for FA-WAP than Com-WAP, which may be attributed to the better release characteristics of the former. These results suggest that the addition of WAP in soil can increase the wetting front advancement rate in the horizontal direction. This observation is in line with the field study conducted by Yang et al. (2015) that reported WAP can effectively contribute to the moisture distribution in point source drip irrigation system due to the higher wetting front advancement rate.

A power curve (Eq. 5) was fitted to the measured wetting front advancement data for quantifying the time duration at which the wetting front touches the farthest end of the cell. The time taken for the wetting front to reach the farthest end of the column was estimated as shown in Fig. 5. It can be noted that in all the cases, the time taken by the wetting front to reach farthest end was faster for FA-WAP compared to Com-WAP.

$$x_f = pt^q \tag{5}$$

In Eq. (5), p and q are two empirical constants, which can be obtained from the regression analysis as indicated in Fig. 5. It was observed that the p parameter is dependent on both WAP

type and soil texture, whereas the q value (=0.5) is constant for the case of water flow through porous medium. A higher value of p parameter denotes a faster wetting front advancement rate. It can be observed that the p value was consistently higher for FA-WAP than Com-WAP. Similarly, the coarse-textured soil exhibited a higher p value than the fine-textured soil considered in this study.

The VWC variation of the soil column with time and distance from the WAP-soil interface is presented in Fig. 6. It is clearly visible that the VWC near the interface quickly increases in the initial stage and approaches a near steady-state value. The results help to affirm that there is continuous water entry and replenishment at the interface (from WAP to soil) even when the wetting front was advancing through the soil. This establishes a continuous release of water from WAP to soil. Irrespective of soil texture, the hydrated FA-WAP resulted in higher VWC at every distance and time compared to Com-WAP. The degree of saturation of the WAP-soil interface remains much below 100% in the case of Com-WAP compared to FA-WAP. This can happen when the outflow of water from the interface is faster than the inflow from WAP. This confirms that the water release from FA-WAP to the soil is faster than Com-WAP. The difference between saturated water content and interface water content reduces with an increase in soil plasticity and clay percentage (Table 1). The degree of saturation of interface is also governed by the difference in negative pore-water pressure between the hydrated WAP and the soil. As the soil plasticity and clay content increase, the soil suction increases. This results in a higher negative pore water pressure of RS as compared to BS and FS. Due to this reason, RS is able to draw water faster from the Com-WAP as compared to the other two soils and reached up to 90% saturation. On the other hand, the WAP-soil interface of all soil textures reached the near-saturated state (Degree of saturation > 95%) in the case of FA-WAP, which proves the effectiveness of synthesized FA-WAP for quick release and restoration of water content in the soil compared to Com-WAP.

Water release characteristics (WRC) of WAP

The water release kinetics from hydrated WAP of initial thickness of 30 mm in contact with initial dry soil are presented in Fig. 7(a) and (b). The change in GWCs of WAPs were recorded by dismantling the horizontal columns at different time intervals. The WRCs of hydrated WAP to dry soil is different from the kinetics of hydrated WAP to the atmosphere (Fig. 4a). The water release of WAP to initially dry soil is high in the beginning, which progressively decreases. The water release from WAP will continue till the saturation of the entire soil layer and at that point the curve becomes asymptotic with time axis. The water release rate was observed to be higher in FA-WAP than the Com-WAP, which gives an indication that dry soil particles can readily extract water from the former. Among the three soils, the coarse-grained soil (FS) column reached the saturated state in lesser time due to higher water permeability and less water demand (low saturated water content of FS). On the other hand, the fine-grained soil (RS) column absorbed maximum water from hydrated WAP because of its high initial soil suction and saturated water content (i.e., high available storage). The different combinations of soils and WAPs suggests better efficiency of FA-WAP and clay soil for higher WRC if sufficient amount of water is available in WAP.

The water release kinetics was quantified by fitting Eq. (1) to the measured data for both the WAPs. The fitted parameters, kinetic constant (k_1) and characteristic constant (k_2) are reported in Table 6 for all the experimental combinations. It can be observed that the value of kinetic constant (k_1) is exclusively dependent on the WAP type and independent of soil textures considered in this study. Mathematically, a lower value of k_1 parameter suggests higher water release and accordingly FA-WAP has higher water release than Com-WAP. The value of characteristic constant (k_2) depends on soil type and a higher value of k_2 suggest better release of water to the adjacent soil. Moreover, the value of k_2 remains the same for different WAPs and not influenced by WAP type. These characteristics were consistent for WAP exposed to

the atmosphere as listed in Table 4. Therefore, the kinetic equation parameters serve as unique values for quantifying the WRC of a given WAP-soil combination.

The water release rate from both WAPs to dry soils were further calculated using Eq. (2) for a better understanding of WRC and presented in Fig. 7(c)-(e). It can be observed that the initial water release rate from Com-WAP is quite less than FA-WAP for all the soil samples. This indicates that FA-WAP was able to release water quickly to the WAP-soil interface and the released water was further migrated to the remaining part of the soil column. The water release rate from both WAPs was found to be almost similar after 8 hrs, 10 hrs, and 10.5 hrs from the beginning of the test in the case of FS, BS, and RS, respectively. These observations suggested better performance of FA-WAP as compared to Com-WAP in terms of water release rate to dry soils.

The above discussion further indicates that there was adequate water stored in the WAP (30 mm thick hydrated WAP) for the soil column to approach near saturation. However, the water release curve with 30 mm thick layer of hydrated WAP does not give clear indication about the water release into a soil with limited water availability. In case of extreme drying conditions, it is important to ensure that maximum amount of stored water inside WAP network is released back to soil. Therefore, it is necessary to understand the performance of both WAPs when limited amount of water is available inside the WAP network. For this purpose, the water release characteristics of hydrated WAP with initial layer thickness of 20 mm and 10 mm were studied and presented in Fig. 8. It is explicit that an initial hydrated WAP layer thickness of 30 mm is sufficient for all the soils to reach their saturated state. For an initial hydrated Com-WAP layer thickness of 20 mm, FS was able to reach saturated water content, whereas BS and RS exhibited 85% and 74% saturation, respectively. This is expected due to the low porosity of FS as listed in Table 3. On the other hand, BS and RS exhibited 91% and 79% saturation, respectively in contact with the 20 mm thick layer of FA-WAP.

All the soil samples were found to be well below the saturated state for the initial hydrated WAP layer thickness of 10 mm due to the lower availability of initial water. It can be observed from Fig. 8 that the hydrated Com-WAP achieves a constant GWC of 29 (g/g) from an initial GWC of 279 (g/g) for both BS and RS in the case of 20 mm thick Com-WAP layer. The result indicates that this remaining water stored in the WAP, which is about 10% of its equilibrium water absorbency, could not be transferred to dry soil. Similarly, the final GWC of Com-WAP was close to 28 (g/g) when an initial layer thickness of 10 mm was considered. It is quite clear from the results that about 90% of the absorbed water inside the Com-WAP is available to dry soil. This may be due to the fact that the residual water molecules inside the WAP network are tightly attached to the negatively charged carboxyl group and unavailable for release into the soil. This observation is in good agreement with Yang et al. (2014) that reported higher water availability inside the WAP network may not result in higher water release due to these tightly absorbed water molecules in WAP chain. The final GWC of FA-WAP (with equilibrium water absorbency of 310 g/g) was found to be 9 (g/g) and 8 (g/g) for the layer thickness of 20 mm and 10 mm, respectively, which is only about 3% of its equilibrium water absorbency. This indicates that 97% of the absorbed water is available to dry soil in case of hydrated FA-WAP. Therefore, FA-WAP not only absorbs higher amount of water due to its higher water absorbency but also releases higher percentage of the absorbed water into the dry soil. This is an essential parameter for utilization of WAP where sufficient amount of water may not be available for full hydration. Based on these observations on limited water availability in WAP, it can be concluded that the laboratory synthesized FA-WAP is more advantageous than Com-WAP under water stress conditions considering the water release characteristics.

Summary and conclusions

The use of water absorbing polymer (WAP) for preserving soil moisture under extreme drought conditions necessitates the quantification of water release characteristics of WAPs to initially dry soils. The water release from WAPs to ambient atmosphere was characterized through evaporation experiments. The water release behaviour of a commercially available WAP (Stockosorb) and a FA-WAP (fly ash modified WAP) were studied in three different soils of varying particle size distribution and plasticity. The water release curves of the WAPs were established by performing absorption tests using horizontal soil column test setup in two different initial conditions of WAPs, including fully hydrated condition (i.e., sufficient water available inside WAP to achieve 100% saturation of soil) and limited water availability condition. The following conclusions were drawn from the present study,

i) The rate of evaporation affect the efficiency of WAP when used in soils. The rate of water evaporation from FA-WAP to the atmosphere was found to be slower compared to the Com-WAP due to the lower kinetic constant (k_1) of the former.

ii) In case of the WAPs directly in contact with dry soils and the exposure time remaining the same, the wetting front advancement in the soils was faster with FA-WAP compared to the Com-WAP. The degree of saturation attained by the soils in contact with the FA-WAP was found to be higher (>95%) as compared to that with the Com-WAP, in which case the degree of saturation of the soils remained between 74% and 90%. The difference in the wetting front advancement is governed by the release characteristics of WAP and the negative pore-water pressure of dry soil.

iii) The water release rate from WAPs to dry soils was found to be higher for the FA-WAP irrespective of the soil types considered in this study. The fine-grained soils used in this study (silt loam and clay loam) were found to draw more water from the WAPs as compared to the sand. The combination of the FA-WAP and the clay loam was found to be more efficient in terms of water release rate, particularly so when the WAP was fully saturated.

iv) The WAPs studied were found to release water to dry soils even under limited water availability conditions. About 90% of the absorbed water from Com-WAP and about 97% of the absorbed water from FA-WAP was found to be released to the dry soils. This indicates that partially hydrated WAPs can release the stored water to adjacent soils, and the amount depends on the characteristics of the WAP and the interacting soil.

The present study is the first to examine the water release characteristics (WRCs) of WAPs with different compositions when interacting with different soil types (sand, silt loam, and clay loam). The findings from the study suggested that the total absorbed water in WAP network is not available to dry soil even under water stress conditions, and the amount of water released depends on the WAP type. Therefore, the WRC of WAP in both fully hydrated condition and limited water availability condition govern the selection of WAPs to mitigate water stress in soil. The study is a stepping stone for creating a database of different WAP-soil combinations that can serve as a guideline for the selection of suitable WAPs for various geoenvironmental and agricultural applications.

Acknowledgments

The authors thankfully acknowledge Department of Biotechnology (DBT), India for the financial support through funded research project BT/PR45283/NER/95/1919/2022 registered at Indian Institute of Technology Guwahati. The authors would also like to thank the Central Instrument Facility (CIF) and Department of Chemistry, Indian Institute of Technology Guwahati for providing the necessary support required for this research work.

Data Availability Statement

Some or all data, models, or code that support the findings of this study are available from the corresponding author upon reasonable request.

References

Adjuik, T. A., S. E. Nokes, M. D. Montross, R. Walton, O. Wendroth. 2022. “Laboratory determination of the impact of incorporated alkali lignin-based hydrogel on soil hydraulic conductivity.” *Water* 14(16): 2516. https://doi.org/10.3390/w14162516

ASTM (American Society for Testing and Materials). 2007. Standard test method for particle-size analysis of soils. ASTM D422-63. West Conshohocken, PA: ASTM international.

ASTM (American Society for Testing and Materials). 2014. Standard test method for specific gravity of soil solids by water pycnometer. ASTM D854. West Conshohocken, PA: ASTM international.

ASTM (American Society for Testing and Materials). 2015. Standard Test Method for Measurement of Hydraulic Conductivity of Porous Material Using a Rigid-Wall, Compaction-Mold Permeameter. ASTM D5856. West Conshohocken, PA: ASTM international.

ASTM (American Society for Testing and Materials). 2017a. Standard practice for classification of soils for engineering purposes (unified soil classification system). ASTM D2487. West Conshohocken, PA: ASTM international.

ASTM (American Society for Testing and Materials). 2017b. Standard test methods for liquid limit, plastic limit, and plasticity index of soils. ASTM D4318. West Conshohocken, PA: ASTM international.

ASTM (American Society for Testing and Materials). 2018. Standard Test Method for Measuring the Exchange Complex and Cation Exchange Capacity of Inorganic Fine-Grained Soils. ASTM D7503. West Conshohocken, PA: ASTM international.

Bo, Z., L. Renkuan, L. Yunkai, G. Tao, Y. Peiling, F. Ji, X. Weimin, Z. Zhichao. 2012. “Water-absorption characteristics of organic–inorganic composite superabsorbent polymers and its effect on summer maize root growth.” *Journal of Applied Polymer Science* 126(2): 423-435. https://doi.org/10.1002/app.36652

Bordoloi, S., J. Ni, C. W. W. Ng. 2020. “Soil desiccation cracking and its characterization in vegetated soil: A perspective review.” *Science of the Total Environment* 729: 138760. https://doi.org/10.1016/j.scitotenv.2020.138760

Bruce, R. R., A. Klute. 1956. “The measurement of soil moisture diffusivity.” *Soil Science Society of America Journal* 20(4): 458-462. https://doi.org/10.2136/sssaj1956.03615995002000040004x

Cao, Y., B. Wang, H. Guo, H. Xiao, T. Wei. 2017. “The effect of super absorbent polymers on soil and water conservation on the terraces of the loess plateau.” *Ecological Engineering* 102: 270-279. https://doi.org/10.1016/j.ecoleng.2017.02.043

Chang, L., L. Xu, Y. Liu, D. Qiu. 2021. “Superabsorbent polymers used for agricultural water retention.” *Polymer Testing* 94: 107021. https://doi.org/10.1016/j.polymertesting.2020.107021

Dehkordi, D. K. 2018. “Effect of Water Quality and Temperature on the Efficiency of Two Kinds of Hydrophilic Polymers in Soil.” *Water Environment Research* 90(6): 490-497. https://doi.org/10.2175/106143017X14839994523389

El-Asmar, J., H. Jaafar, I. Bashour, M. T. Farran, I. P. Saoud. 2017. “Hydrogel banding improves plant growth, survival, and water use efficiency in two calcareous soils.” *Clean–Soil, Air, Water* 45(7): 1700251. https://doi.org/10.1002/clen.201700251

Espejo, A., J. V. Giráldez, K. Vanderlinden, E. V. Taguas, A. Pedrera. 2014. “A method for estimating soil water diffusivity from moisture profiles and its application across an experimental catchment.” *Journal of Hydrology* 516: 161-168. https://doi.org/10.1016/j.jhydrol.2014.01.072

Evangelides, C., G. Arampatzis, C. Tzimopoulos. 2010. “Estimation of soil moisture profile and diffusivity using simple laboratory procedures.” *Soil Science* 175(3): 118-127. https://doi.org/10.1097/SS.0b013e3181d53bb6

Feng, D., B. Bai, C. Ding, H. Wang, Y. Suo. 2014. “Synthesis and swelling behaviors of yeast-g-poly (acrylic acid) superabsorbent co-polymer.” *Industrial & Engineering Chemistry Research* 53(32): 12760-12769. https://doi.org/10.1021/ie502248n

Fredlund, D. G., H. Rahardjo. 1993. Soil mechanics for unsaturated soils. USA: John Wiley & Sons.

Hussien, R. A., A. M. Donia, A. A. Atia, O. F. El-Sedfy, A. R. Abd El-Hamid, R. T. Rashad. 2012. “Studying some hydro-physical properties of two soils amended with kaolinite-modified cross-linked poly-acrylamides” Catena 92: 172-178. https://doi.org/10.1016/j.catena.2011.12.010

Kandalai, S., N. J. John, and A. Patel. 2023. “Effects of Climate Change on Geotechnical Infrastructures—state of the art.” *Environmental Science and Pollution Research* 30(7): 16878-16904. https://doi.org/10.1007/s11356-022-24788-7

Krasnopeeva, E. L., G. G. Panova, A. V. Yakimansky. 2022. “Agricultural applications of superabsorbent polymer hydrogels.” *International Journal of Molecular Sciences*, 23(23): 15134. https://doi.org/10.3390/ijms232315134

Lejcuś, K., J. Dąbrowska, D. Garlikowski, M. Śpitalniak. 2015. “The application of water-absorbing geocomposites to support plant growth on slopes.” *Geosynthetics International* 22(6): 452-456. https://doi.org/10.1680/jgein.15.00025

Liu, B., C. S. Tang, X. H. Pan, C. Zhu, Y. J. Cheng, J. J. Xu, B. Shi. 2021. “Potential Drought Mitigation Through Microbial Induced Calcite Precipitation-MICP.” *Water Resources Research* 57(9): e2020WR029434. https://doi.org/10.1029/2020WR029434

Liu, X., H. Zhao, Y. He, X. Zhao, T. Zhang, Y. Li. 2009. “Water diffusivity of sandy soil of different particle sizes in typical sandy cropland.” In: Environmental Science and Information Application Technology, 2: 335–338. https://doi.org/10.1109/ESIAT.2009.368

Marczak, D., K. Lejcuś, G. Kulczycki, J. Misiewicz. 2022. “Towards circular economy: Sustainable soil additives from natural waste fibres to improve water retention and soil fertility.” *Science of the Total Environment* 844: 157169. https://doi.org/10.1016/j.scitotenv.2022.157169

Mignon, A., N. De Belie, P. Dubruel, S. Van Vlierberghe. 2019. “Superabsorbent polymers: A review on the characteristics and applications of synthetic, polysaccharide-based, semi-synthetic and ‘smart’ derivatives.” *European Polymer Journal* 117: 165-178. https://doi.org/10.1016/j.eurpolymj.2019.04.054

Narjary, B., P. Aggarwal, A. Singh, D. Chakraborty, R. Singh. 2012. “Water availability in different soils in relation to hydrogel application.” *Geoderma* 187: 94-101. https://doi.org/10.1016/j.geoderma.2012.03.002

Ni, J., Z. T. Wang, X. Geng. 2024. “Vegetation growth promotion and overall strength improvement using biopolymers in vegetated soils.” *Canadian Geotechnical Journal* 61(7): 1294-1310. https://doi.org/10.1139/cgj-2022-0049

Peleg, M. 1988. “An empirical model for the description of moisture sorption curves.” *Journal of Food science* 53(4): 1216-1217. https://doi.org/10.1111/j.1365-2621.1988.tb13565.x

Piqué, T. M., D. Manzanal, M. Codevilla, S. Orlandi. 2019. “Polymer-enhanced soil mixtures for potential use as covers or liners in landfill systems.” *Environmental Geotechnics* 8(7): 467-479. https://doi.org/10.1680/jenge.18.00174

Pk, S., R. Bashir, R. Beddoe. 2018. “Effect of climate change on earthen embankments in Southern Ontario, Canada.” *Environmental Geotechnics* 8(2): 148-169. https://doi.org/10.1680/jenge.18.00068

Rodrigues, F. H., A. R. Fajardo, A. G. Pereira, N. M. Ricardo, J. Feitosa, E. C. Muniz. 2012. “Chitosan-graft-poly (acrylic acid)/rice husk ash based superabsorbent hydrogel composite:

preparation and characterization." *Journal of Polymer Research* 19(12): 1-10. https://doi.org/10.1007/s10965-012-0001-8

Saha, A., B. Rattan, S. Sreedeep, U. Manna. 2020a. "Quantifying the interactive effect of water absorbing polymer (WAP)-soil texture on plant available water content and irrigation frequency." *Geoderma* 368: 114310. https://doi.org/10.1016/j.geoderma.2020.114310

Saha, A., B. Rattan, S. Sreedeep, U. Manna. 2021b. "Quantifying the combined effect of pH and salinity on the performance of water absorbing polymers used for drought management." *Journal of Polymer Research* 28(11): 1-14. https://doi.org/10.1007/s10965-021-02795-5

Saha, A., C. B. Gupt, S. Sreedeep. 2021a. "Recycling Natural Fibre to Superabsorbent Hydrogel Composite for Conservation of Irrigation Water in Semi-arid Regions." Waste and Biomass Valorization 12(12): 6433-6448. https://doi.org/10.1007/s12649-021-01489-9

Saha, A., S. Sreedeep, U. Manna. 2020b. "Superabsorbent hydrogel (SAH) as a soil amendment for drought management: A review." *Soil and Tillage Research* 204: 104736. https://doi.org/10.1016/j.still.2020.104736

Saha, A., S. Sreedeep, U. Manna. 2021c. "Predictive model for water retention curve of water-absorbing polymer amended soil." *Géotechnique Letters* 11(3): 164-170. https://doi.org/10.1680/jgele.21.00015

Saha, A., S. Sreedeep, U. Manna. 2022a. "Hysteresis Model for Water Retention Characteristics of Water-Absorbing Polymer-Amended Soils." *Journal of Geotechnical and Geoenvironmental Engineering* 148(4): 04022008. https://doi.org/10.1061/(ASCE)GT.1943-5606.0002764

Saha, A., S. Sreedeep, U. Manna. 2022b. "Characterization of Moisture Movement in Water Absorbing Polymer-Soil System: A Horizontal Absorption Method." *Journal of Materials in Civil Engineering* 34(10): 04022270. https://doi.org/10.1061/(ASCE)MT.1943-5533.0004422

Saha, A., S. Sreedeep, U. Manna, L. Sahoo. 2020c. “Transformation of non-water sorbing fly ash to a water sorbing material for drought management.” *Scientific Reports* 10(1): 1-16. https://doi.org/10.1038/s41598-020-75674-6

Sarmah, D., N. Karak. 2020. “Biodegradable superabsorbent hydrogel for water holding in soil and controlled-release fertilizer.” *Journal of Applied Polymer Science* 137(13): 48495. https://doi.org/10.1002/app.48495

Shah, L. A., M. Khan, R. Javed, M. Sayed, M. S. Khan, A. Khan, M. Ullah. 2018. “Superabsorbent polymer hydrogels with good thermal and mechanical properties for removal of selected heavy metal ions.” *Journal of Cleaner Production* 201: 78-87. https://doi.org/10.1016/j.jclepro.2018.08.035

Spagnol, C., F. H. Rodrigues, A. G. Neto, A. G. Pereira, A. R. Fajardo, E. Radovanovic, A. F. Rubira, E. C. Muniz. 2012. “Nanocomposites based on poly (acrylamide-co-acrylate) and cellulose nanowhiskers.” *European Polymer Journal* 48(3): 454-463. https://doi.org/10.1016/j.eurpolymj.2011.12.005

Śpitalniak, M., K. Lejcuś, J. Dąbrowska, D. Garlikowski, A. Bogacz. 2019. “The influence of a water absorbing geocomposite on soil water retention and soil matric potential.” *Water* 11(8): 1731. https://doi.org/10.3390/w11081731

Van Genuchten, M. T. 1980. “A closed-form equation for predicting the hydraulic conductivity of unsaturated soils.” *Soil Science Society of America Journal* 44(5): 892-898. https://doi.org/10.2136/sssaj1980.03615995004400050002x

Vardon, P. J. 2015. “Climatic influence on geotechnical infrastructure: a review.” *Environmental Geotechnics* 2(3): 166-174. https://doi.org/10.1680/envgeo.13.00055

Villarreal, R., L. A. Lozano, E. M. Melani, M. P. Salazar, M. F. Otero, C. G. Soracco. 2019. "Diffusivity and sorptivity determination at different soil water contents from horizontal infiltration." *Geoderma* 338: 88-96. https://doi.org/10.1016/j.geoderma.2018.11.045

Yang, B., K. Xu, Z. Zhang. 2020a. "Mitigating evaporation and desiccation cracks in soil with the sustainable material biochar." *Soil Science Society of America Journal* 84(2): 461-471. https://doi.org/10.1002/saj2.20047

Yang, F., R. Cen, W. Feng, J. Liu, Z. Qu, Q. Miao. 2020b. "Effects of super-absorbent polymer on soil remediation and crop growth in arid and semi-arid areas." *Sustainability* 12(18): 7825. https://doi.org/10.3390/su12187825

Yang, L., Y. Han, P. Yang, C. Wang, S. Yang, S. Kuang, H. Yuan, C. Xiao. 2015. "Effects of superabsorbent polymers on infiltration and evaporation of soil moisture under point source drip irrigation." *Irrigation and Drainage* 64(2): 275-282. https://doi.org/10.1002/ird.1883

Yang, L., Y. Yang, Z. Chen, C. Guo, S. Li. 2014. "Influence of super absorbent polymer on soil water retention, seed germination and plant survivals for rocky slopes eco-engineering." *Ecological Engineering* 62: 27-32. https://doi.org/10.1016/j.ecoleng.2013.10.019

Zhao, J., X. Qiu, X. Liu, X. Ye, H. Xiong, Y. Liang, Z. Lei. 2021. "Preparation and anti-evaporation properties of organic–inorganic superabsorbent based on Tragacanth gum and clay." *Journal of Applied Polymer Science* 138(32): 50777. https://doi.org/10.1002/app.50777

Table 1. Basic physical properties of the soils

Physical Properties		Fine Sand	Brahmaputra Soil	Red Soil
Designation		FS	BS	RS
Specific Gravity (G)		2.66	2.73	2.69
Grain Size Distribution (%)	Gravel (> 4.75 mm)	0	0	0
	Coarse sand (2 mm – 4.75 mm)	14	0	0
	Medium sand (0.425 mm – 2 mm)	40	0	6
	Fine sand (0.075 mm – 0.425 mm)	46	32	19
	Silt (0.002 mm – 0.075 mm)	0	58	47
	Clay (< 0.002 mm)	0	10	28
	Uniformity coefficient (C_u)	6.2	2	NA
	Coefficient of curvature (C_c)	1.3	4.1	NA
Liquid limit (LL)		NA	31	40
Plastic limit (PL)		NA	21	19
Plasticity Index (PI) [%]		NA	10	21
Cation exchange capacity (meq/100 g)		NA	3	10
USCS Classification		SP	CL	CL
USDA Classification		Sand	Silt Loam	Clay Loam
Minerals present (XRD analysis)		Quartz	Quartz, Calcite	Quartz, Hematite

*NA = Not Applicable/Negligible

Table 2. Basic properties of water absorbing polymers (WAPs)

Parameters		**Com-WAP**	**FA-WAP**
Chemical composition		Crosslinked potassium polyacrylate	Fly ash-crosslinked sodium polyacrylate
Visual appearance		Amorphous granules	Amorphous granules
Particle size (dry)		0.2 mm- 1 mm	0.2 mm- 2 mm
Functional groups (FTIR spectrum)		Hydroxyl (OH), carboxyl (COOH)	Hydroxyl (OH), carboxyl (COOH), Si-O-Si bond
pH		6.0- 7.0	6.5-7.5
Elemental compositions (%) (FESEM-EDX analysis)	C	42.8 ± 1.1	49.8 ± 1.9
	O	36.8 ± 0.9	36.4 ± 1.5
	K	10.1 ± 0.8	0.5 ± 0.4
	N	8.4 ± 0.6	2.1 ± 3.1
	Na	0.8 ± 0.1	4.7 ± 0.3
	Si	0.2 ± 0.3	2.1 ± 0.1
	Ca	0	2.0 ± 0.2
	Al	0	1.1 ± 0.1
	Fe	0	0.9 ± 0.3
Equilibrium water-absorbing capacity (g/g)		279	310
Equilibrium swelling time (hrs)		1.5	4

Table 3. Details of the initial compaction state of soils packed in column

Parameters	Fine Sand	Brahmaputra Soil	Red Soil
Bulk density (g/cc)	1.8	1.75	1.6
Dry density (g/cc)	1.78	1.7	1.5
Void ratio (*e*)	0.49	0.61	0.79
Porosity (*n*)	0.33	0.38	0.44

Table 4. Details of the desorption kinetic model parameters for WAPs dried at constant temperature and humidity (25°C and 50% RH)

Desorption model parameter	Com-WAP	FA-WAP
Kinetic constant (k_1) [hr]	0.8	0.95
Characteristic constant (k_2)	0.0014	0.0015
R^2	0.99	0.99
RMSE (g/g)	6.31	7.53

Table 5. Fitting parameters of evaporation loss characteristic curve (ELCC) for WAP-atmosphere interaction

Fitting parameters	Com-WAP	FA-WAP
ER_s	0.124	0.103
ER_r	0.03	0.03
a (hr^{-1})	0.004	0.002
n	7.25	5.32
m	1.1	5.5

Table 6. Details of the desorption kinetic model parameters for WAPs in contact with dry soil column

Parameters		k_1 (hr)	k_2	R^2	RMSE (g/g)
Fine Sand	Com-WAP	0.06	0.006	0.99	5.31
	FA-WAP	0.024	0.0055	0.99	6.94
Brahmaputra Soil	Com-WAP	0.06	0.0042	0.99	7.27
	FA-WAP	0.024	0.004	0.99	3.94
Red Soil	Com-WAP	0.06	0.0037	0.99	5.97
	FA-WAP	0.024	0.0035	0.99	5.31

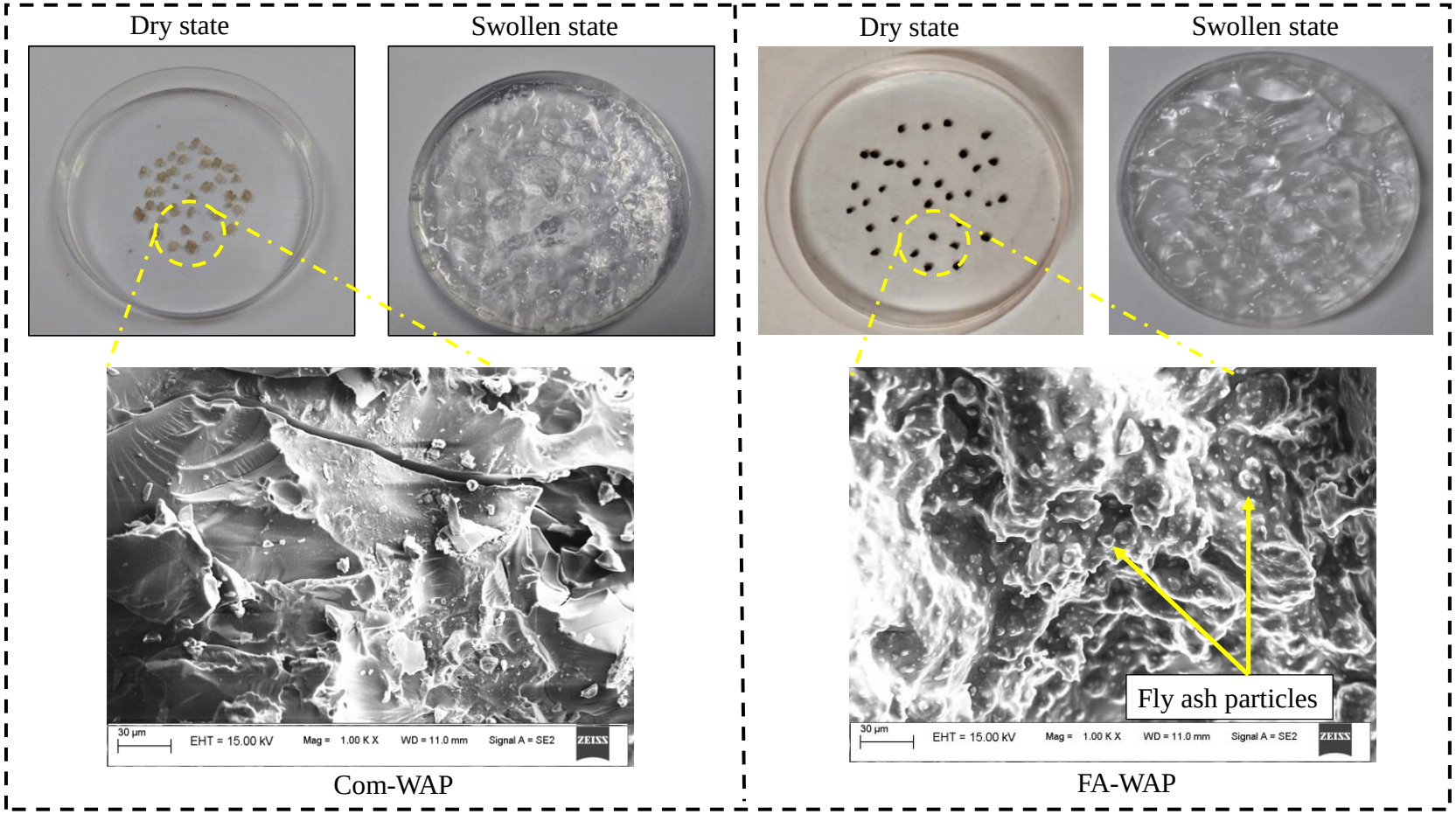

Fig. 1. Pictorial view of the dry and swollen WAPs with the surface morphology (at 1000X magnification)

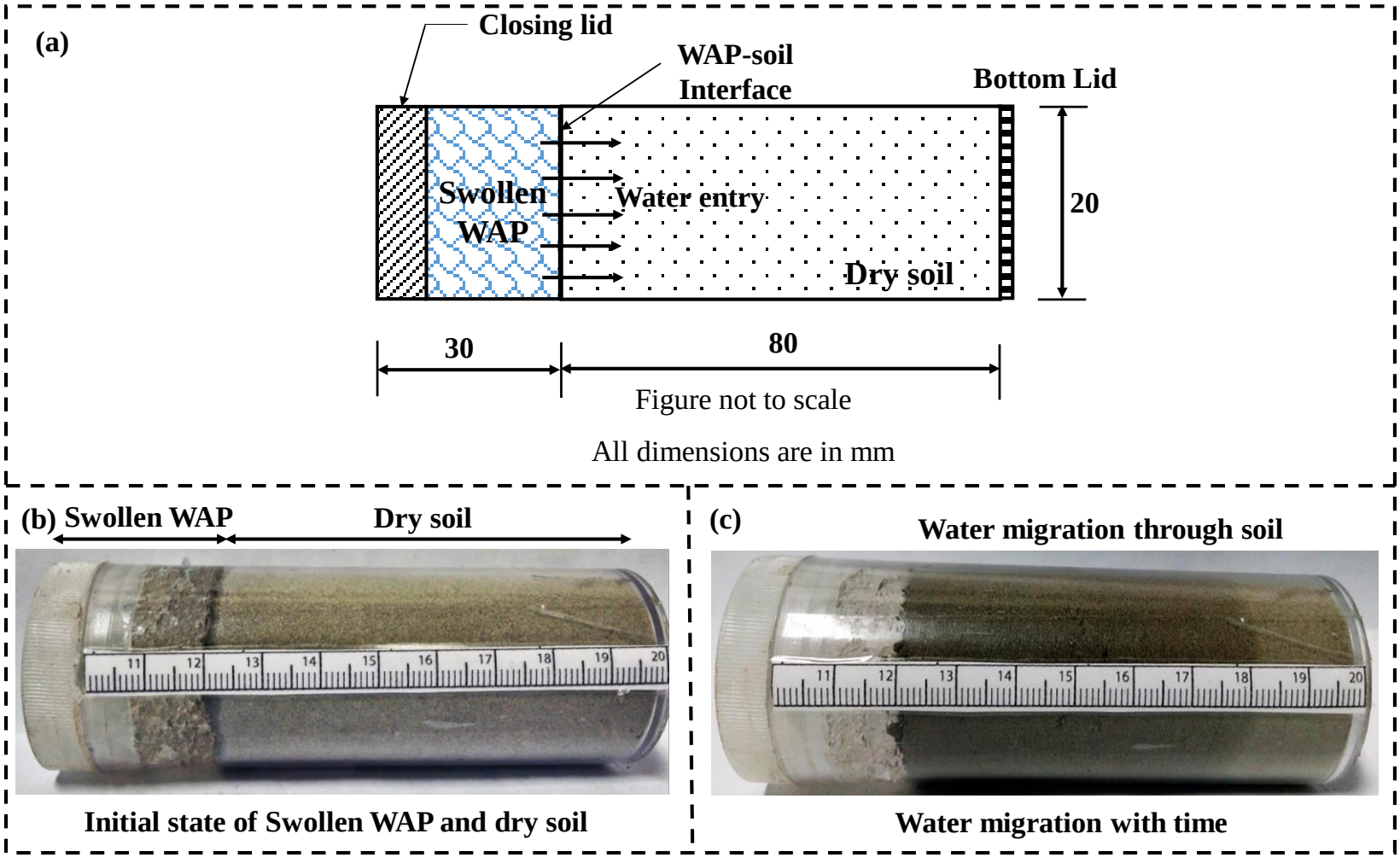

Fig. 2. (a) Horizontal soil column test (HSCT) set up and soil column (b) at initial state and (c) after 24 hours

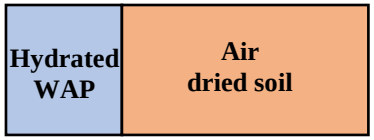

(a) Initial condition (time t = 0)
Swollen WAP in contact with air dried soil

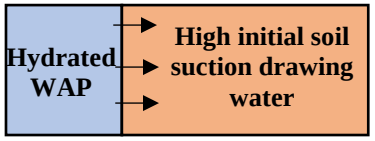

(b) At time t = t_1
At air dry state, soil suction is high
This draws water into the soil at the interface

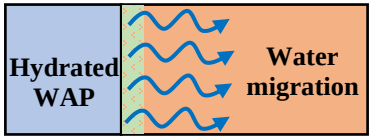

High saturation zone near interface

(c) At time t = t_2
Water entering into the soil is redistributed

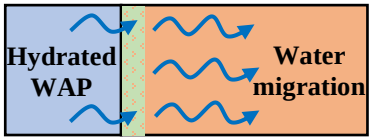

(d) At time t = t_3
Higher water migration reduces saturation at the interface causing further water entry

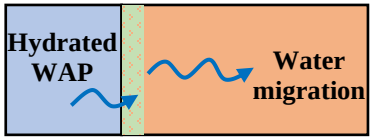

(e) At time t = t_4
As soil saturation increases suction gradient reduces at the interface
The water entry from swollen WAP reduces

Fig. 3. Conceptual understanding of water release mechanism from hydrated WAP to initially dry soil

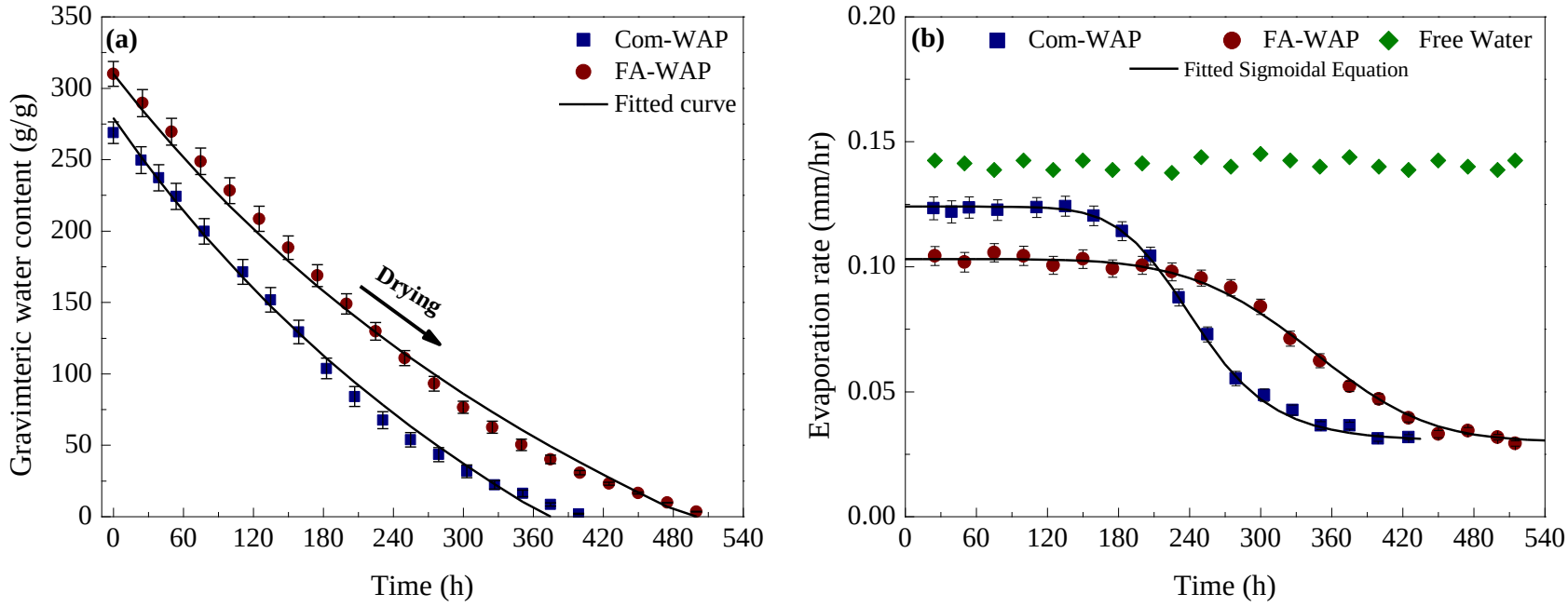

Fig. 4. (a) Water release kinetics and (b) variation of evaporation rate with time for hydrated WAP exposed to atmosphere

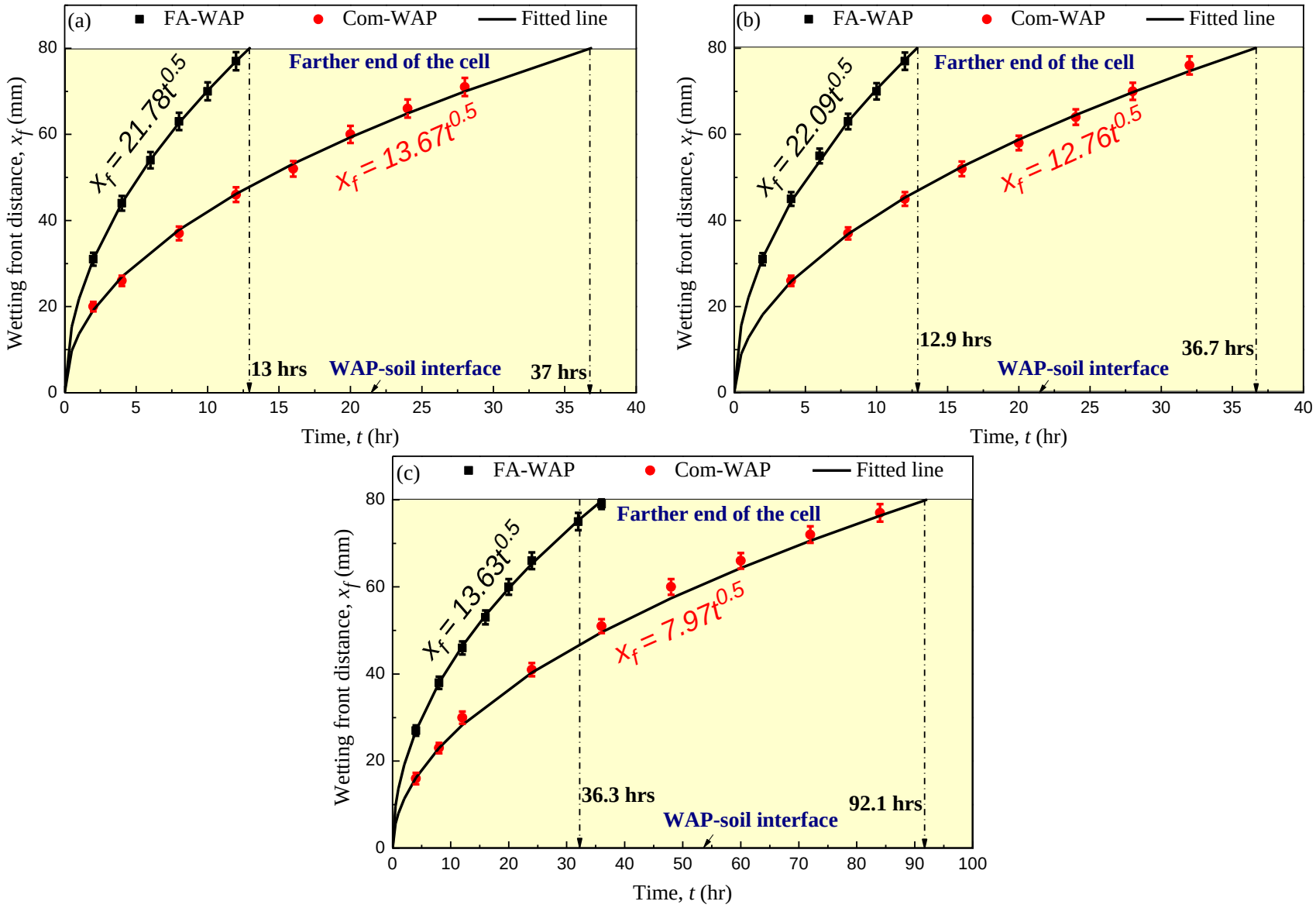

Fig. 5. Wetting front advancement through (a) FS, (b) BS, and (c) RS in contact with the hydrated WAP

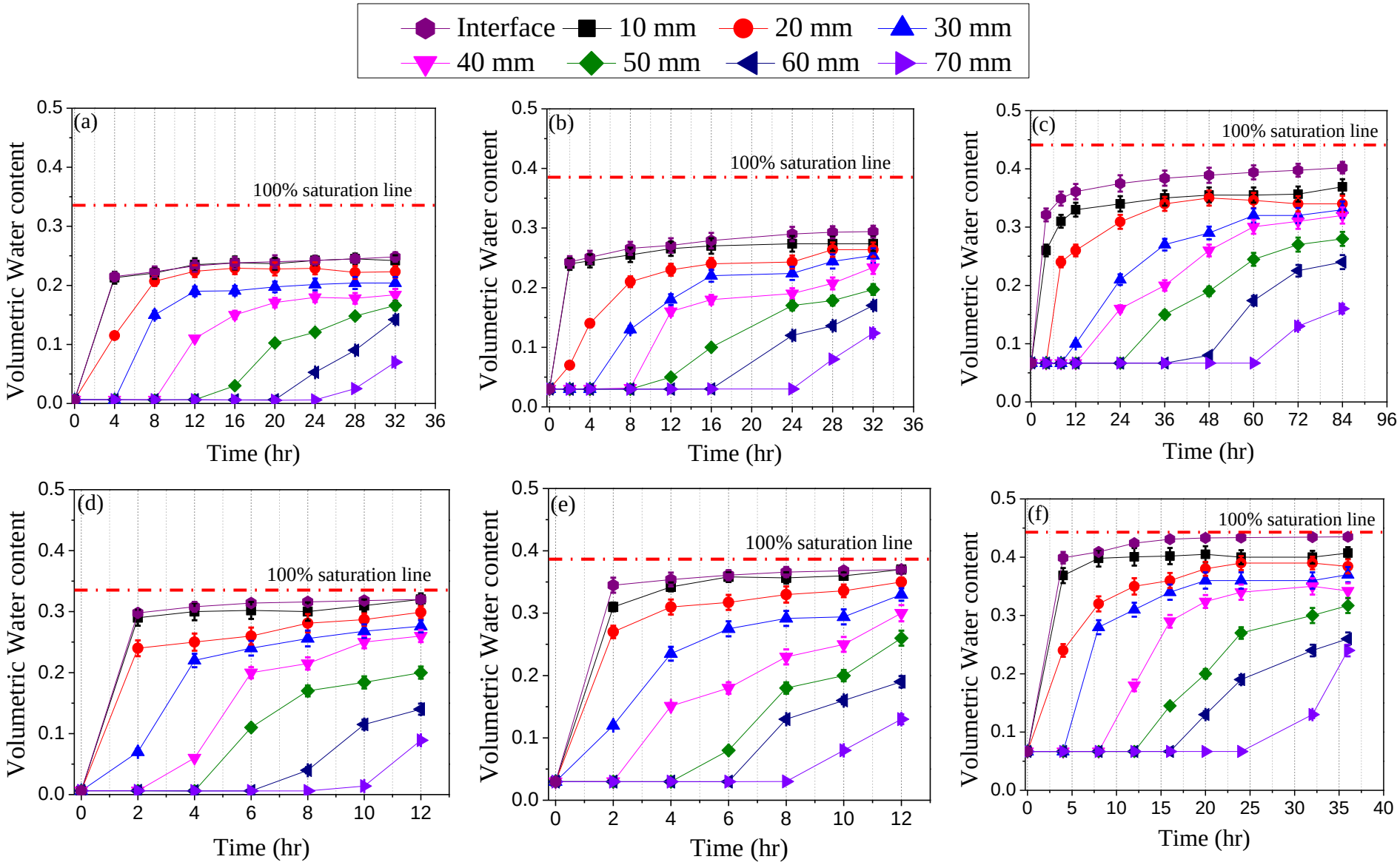

Fig. 6. Volumetric water content-time variation at different distances from the WAP-soil interface for (a) FS, (b) BS, (c) RS with Com-WAP and (d) FS, (e) BS, (f) RS with FA-WAP

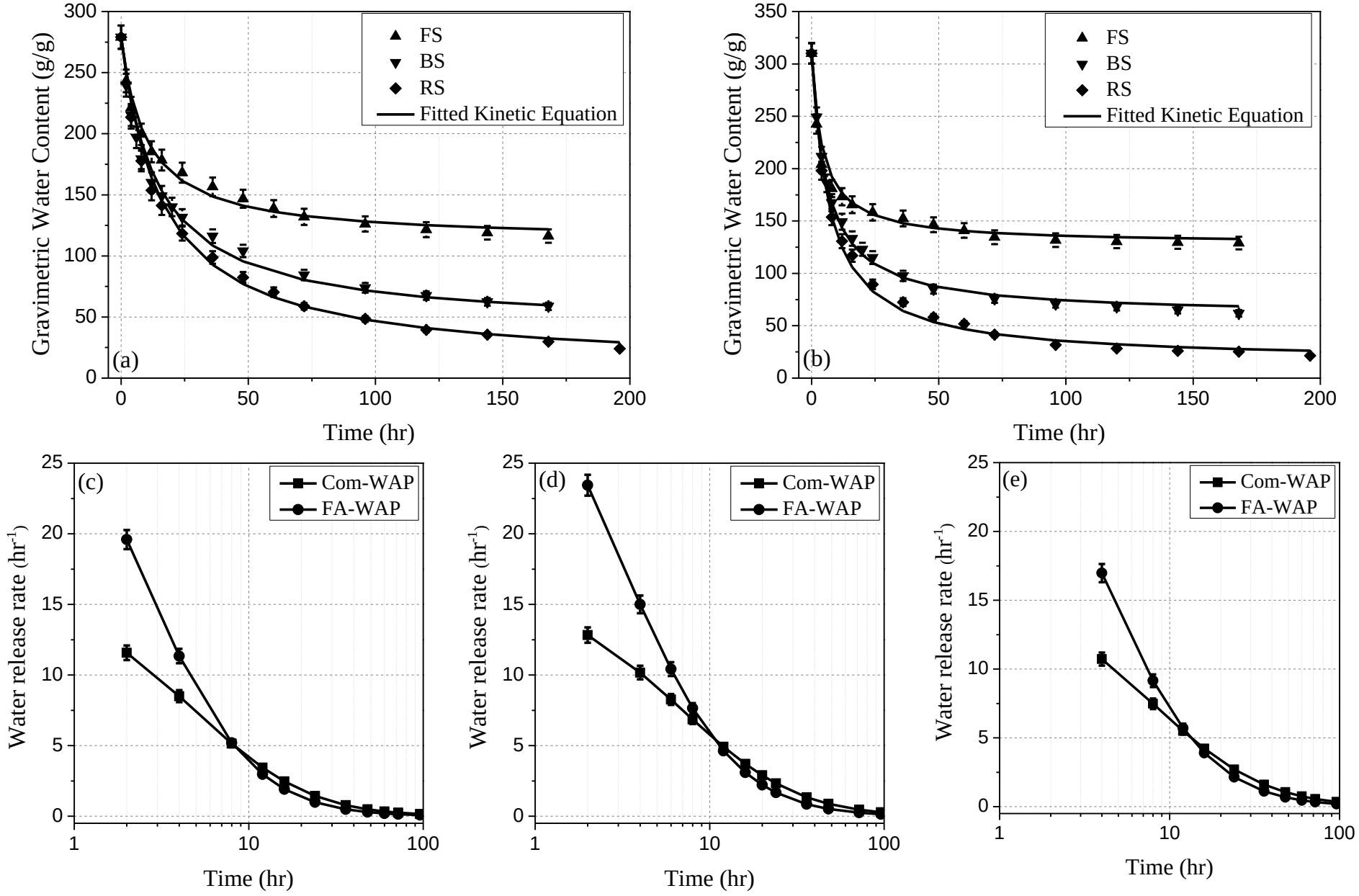

Fig. 7. Water release kinetics of for Com-WAP in contact with (a) FS, (b) BS, (c) RS and FA-WAP in contact with (d) FS, (e) BS, (f) RS

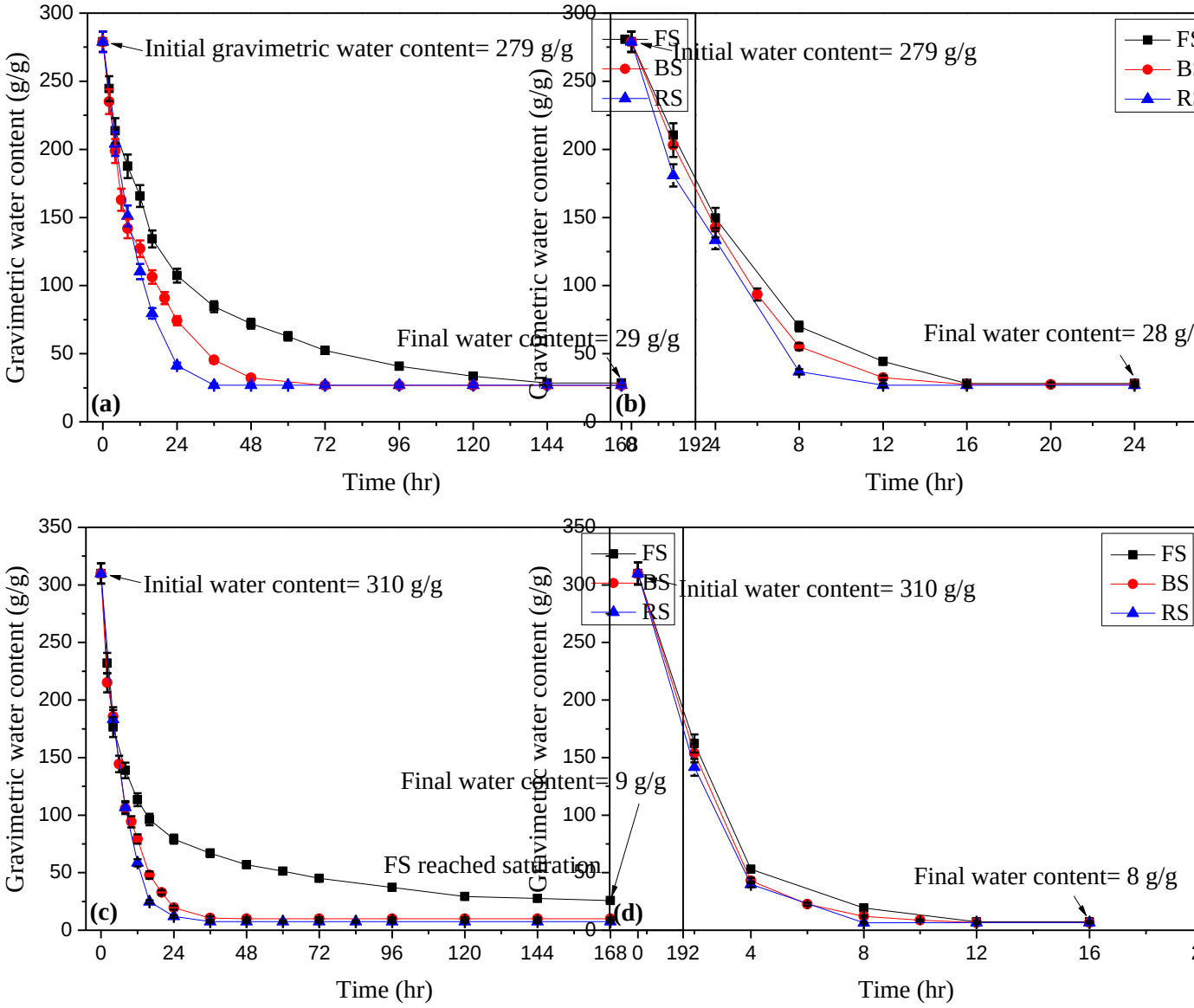

Fig. 8. WRC (water release characteristics) of (a) 20 mm thick layer of Com-WAP, (b) 10 mm thick layer of Com-WAP, (c) 20 mm thick layer of FA-WAP and (d) 10 mm thick layer FA-WAP